Intercalation stage dependence of core electronic excitations in Li-intercalated graphite from inelastic X-ray scattering

G. E. Stutz, M. Otero, S. A. Ceppi, C. B. Robledo, G. Luque, E. Leiva, and D. E. Barraco Díaz

Citation: Appl. Phys. Lett. **110**, 253901 (2017); doi: 10.1063/1.4986922
View online: http://dx.doi.org/10.1063/1.4986922
View Table of Contents: http://aip.scitation.org/toc/apl/110/25
Published by the American Institute of Physics

Intercalation stage dependence of core electronic excitations in Li-intercalated graphite from inelastic X-ray scattering

G. E. Stutz,[1,2,a)] M. Otero,[3,4] S. A. Ceppi,[1,2] C. B. Robledo,[3,4] G. Luque,[3,4] E. Leiva,[3,4] and D. E. Barraco Díaz[1,2]

[1]*Facultad de Matemática, Astronomía, Física y Computación (FaMAF), Universidad Nacional de Córdoba (UNC), Córdoba 5000, Argentina*
[2]*IFEG, CONICET–UNC, FaMAF, Córdoba 5000, Argentina*
[3]*Departamento de Química Teórica y Computacional, Facultad de Ciencias Químicas (FCQ), Universidad Nacional de Córdoba, Córdoba 5000, Argentina*
[4]*INFIQC, CONICET–UNC, FCQ, Córdoba 5000, Argentina*

(Received 12 April 2017; accepted 7 June 2017; published online 19 June 2017)

Li and C 1*s* core-electron excitation spectra of electrochemically prepared stage-II and stage-I lithiated graphite were investigated by means of inelastic X-ray scattering spectroscopy. The near-edge structure is discussed, and the spectral features are interpreted using *ab initio* calculations. Our results confirm the invariance of the excitation threshold for transitions from C 1*s* core-states to empty π^* states upon Li intercalation for stage-I and show this invariance also occurs for the second stage of intercalation. A systematic shift of the σ^* excitation threshold to lower energies with the Li content was observed. The Li core spectra reveal an ionic character of the intercalated Li in stage-I and in stage-II. The present results provide further valuable information for forthcoming *in situ* studies of lithiation/delithiation processes in graphite anodes by inelastic X-ray scattering spectroscopy. *Published by AIP Publishing*. [http://dx.doi.org/10.1063/1.4986922]

Rechargeable lithium-ion batteries have become the most important electrochemical energy storage system of portable electronic devices and emerge as the preferred energy source for electric vehicles.[1] Graphite is still the most commonly used material for anodes in Li-ion batteries.[2] During the charging/discharging cycles, lithium is intercalated/deintercalated from the graphitic layers of the anode, and different staged intercalation compounds are sequentially formed.[3,4]

The electronic structure of graphite intercalation compounds, in particular, lithium intercalated graphite (LIG), has attracted much attention and has been the subject of several theoretical and experimental studies in the last decade. While theoretical studies of LIG have been performed at different intercalation stages,[5,6] core-level spectroscopic techniques have been applied almost exclusively to LIG at the first stage of intercalation (LiC_6).[7–17] Reported spectroscopic studies on higher intercalation stages (Li_xC_6, $x < 1$) are very scarce.[18] Most of the experimental studies were carried out on chemically prepared samples, whereas only a few studies[7–10] were conducted on electrochemically lithiated samples, which are more relevant from a technological point of view. Early theoretical[5] and experimental[16,17] studies already established the ionic nature of intercalated lithium in graphite in the first stage of intercalation. Further evidence in this direction has been provided by more recent theoretical[6] and experimental core-level spectroscopic[7,8] works. Raman spectroscopy has proven to be a powerful tool to perform *in situ* characterization of an intercalation stage in carbon-based anode materials.[19] Shifts of the *G* band in the Raman spectrum provide additional evidence for charge transfer effects during Li intercalation.[20]

A deep understanding of the dynamic of the lithiation/delithiation mechanism of the graphite anode in Li-ion batteries is of fundamental importance to propose improvements to Li-ion cells. Hard X-ray-based inelastic scattering (IXS) spectroscopy yields true bulk information on electronic excitation and structure and is compatible with various sample environments,[21] circumventing the shortcomings of UV/soft X-ray spectroscopies. Recent developments of multi-crystal spectrometers[22] will make it feasible to carry out *in situ* studies of Li-ion batteries by means of IXS in the near future. Fundamental groundwork for such studies was established from *ex situ* IXS experiments[8] but limited to stage-I LIG samples. That study demonstrated the compatibility of the IXS technique with electrochemically prepared samples. Nevertheless, there are some controversial results between the two existing IXS studies[8,12] on stage-I LIG in relation to the position of the C 1*s* excitation thresholds, which seem to be the most promising spectroscopic signature for phase identification. In order to shed light on this controversy and to provide further groundwork for future *in situ* studies, we have investigated the near-edge structure of the C and Li core-excitation spectra in stage-I and stage-II LIG by IXS and *ab initio* calculations.

The IXS measurements were performed at the X-ray Diffraction and Spectroscopy (XDS) beamline[23] at the Laboratório Nacional de Luz Síncrotron (LNLS). Scattered radiation at 9.69 keV energy was analyzed by means of a spherical Si(660) crystal operated at a fixed Bragg angle in Rowland geometry. Energy-loss scans were achieved by varying the incident beam energy, which was selected by a sagittally focusing Si(111) double-crystal monochromator. The overall energy resolution was 1.7 eV. LIG samples were prepared electrochemically by lithiating graphite pellets in three electrode cells (sample preparation is described in the

a)Electronic mail: stutz@famaf.unc.edu.ar

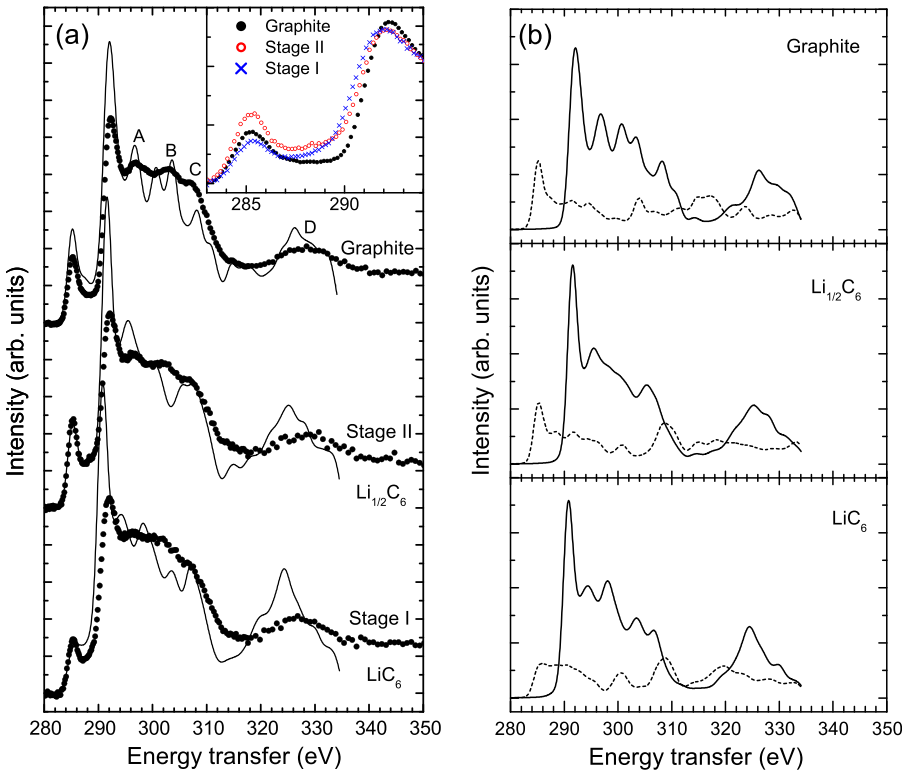

FIG. 1. (a) Experimental C 1*s* IXS spectra of graphite and lithium-intercalated graphite in stage-II and stage-I (symbols). Simulated IXS spectra (see text) for graphite, $Li_{1/2}C_6$ and LiC_6 are also shown (solid lines). For the sake of comparison, the simulated spectra were aligned to the experimental ones, taking the first inflection point as reference energy, and broadened with the experimental energy resolution. In the inset, the experimental near-edge region of the C 1*s* IXS spectra is displayed. (b) Projections of the simulated spectra along directions parallel (dashed line) and perpendicular (solid line) to the *c*-axis.

supplementary material). The LIG sample thickness was selected to be ∼2 mm in order to maximize the scattered intensity for measurements in transmission scattering geometry. The samples were mounted on an He-filled scattering chamber during the IXS measurements. The characteristic golden yellow surface of the stage-I and the reddish surface of the stage-II samples remained unchanged throughout the measurements. The C 1*s* core spectra were measured at a momentum transfer of $q = 1.34$ a.u. In the case of the Li 1*s* core spectra of LIG, in order to reduce the spectral overlap between valence and core contributions without decreasing the scattered intensity to a large extent, a compromise was assumed by setting the magnitude of q to 0.84 a.u. Under these experimental conditions, the interpretation of both IXS core spectra on the basis of dipole-like transitions can be assumed. Experimental IXS spectra by 1*s* electron excitations of C (polycrystalline graphite) and Li metal are shown in Figs. 1 and 2, respectively. The positions

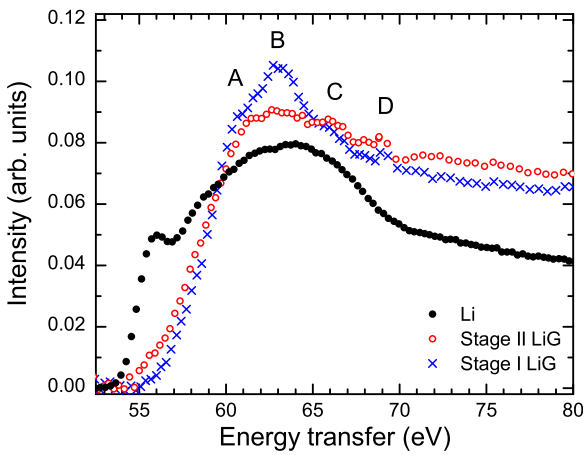

FIG. 2. Li 1*s* IXS spectra of lithium metal (solid circles) and of lithium intercalated in graphite in stage-II (open circles) and stage-I (crosses).

of the 1*s* excitation threshold in pristine graphite (284.37 ± 0.04 eV) and in metallic lithium (54.88 ± 0.03 eV), as determined from the first inflection point of the measured core spectra, were used to check the calibration of the energy-loss scale. The measured C 1*s* threshold position is in good agreement with prior IXS measurements[8] (284 eV). Likewise, the measured Li threshold is in very good agreement with photoyield measurements[24] (54.87 ± 0.05 eV) and also with earlier IXS results (54.8 eV[8] and 55 eV[25]).

C 1*s* IXS spectra of stage-I and stage-II LIG are shown in Fig. 1. They exhibit the two typical absorption thresholds of graphite, corresponding to electronic transitions from the 1*s* core level to π^* (lower energy threshold) and to σ^* (higher energy threshold) empty states. Present measurements show that the threshold for $1s \rightarrow \pi^*$ transitions remains unchanged upon Li intercalation within the experimental uncertainties (-0.04 ± 0.07 eV and -0.03 ± 0.03 eV for stage-I and stage-II, respectively), while the threshold for $1s \rightarrow \sigma^*$ transitions shifts by -0.58 ± 0.09 eV and by -0.15 ± 0.05 eV for stage-I and stage-II LIG, respectively. Our results for stage-I LIG are in accordance with the IXS measurements from Ref. 8, where an invariance of the π^* threshold and a shift of the σ^* threshold of -0.6 ± 0.1 eV were measured. On the contrary, in the early IXS study[12] on stage-I lithiated HOPG, the σ^* excitation threshold was observed to remain invariant upon lithiation. Further evidence for the invariance of the onset energy of the C *K*-edge and for a slight shift of the σ^* excitation threshold to lower energies was provided by an EELS study on first-stage lithiated graphite.[10] Calculations of the electron energy-loss near-edge structure (ELNES) spectra of different LIG systems also predicted a shift of the onset of $1s \rightarrow \sigma^*$ excitations towards lower energies.[6]

The measured σ^* threshold of stage-II LIG lies between those of graphite and stage-I LIG (see inset in Fig. 1). This

trend is consistent with the fact that on average over all C sites, the electron bands of LIG should approximate that of pure graphite at higher intercalation stages. The shift of the σ^* threshold and the observed trend with the lithiation stage could be a consequence of the change in the screening of the Coulomb potential induced by the relocalization of the Li conduction electrons to regions around the C atoms in the LIG systems, as pointed out in Ref. 6. The shift of the σ^* threshold in stage-I LIG, as induced by the increase in the C–C bond length,[8] was ruled out by Titantah *et al.*,[6] at least as a dominant effect, on the basis of a theoretical study on changes in the ELNES spectra with the bond length in carbon systems.[26] The cause of the invariance of the π^* threshold upon Li intercalation may be a combined effect of different lithiation-stage-dependent factors other than the shift of the Fermi level due to the charge transfer from the Li $2s$ states to graphite π^* states. Among such factors, the shape of the density of states at the onset of the unoccupied states and screening and core-hole effects should be considered. A comprehensive theoretical study of the influence of those factors on the π^* threshold would yield relevant insights into the understanding of the experimental findings.

Above the excitation thresholds, some fine structures, which show a weak dependence on the lithiation stage, can be distinguished in the measured IXS spectra. In the graphite spectrum, three small peaks at 297, 303, and 307 eV (labeled A, B, and C, respectively, in Fig. 1) and an additional, broad peak (labeled as D) at higher energies (328 eV) are clearly visible. In the spectra of stage-II and stage-I LIG, similar features are present. The features A, B, and C shift slightly to lower energies and lose spectral weight for the increasing Li content. The C $1s$ absorption spectra of graphite and of Li_xC_6 ($x = 1/2, 1$) were calculated using the XSPECTRA calculation code[27] within the Quantum Expresso package[28] (calculation details are provided in the supplementary material). The absorption cross section was related to the IXS cross section according to Ref. 25. The simulated IXS spectra (see Fig. 1) reproduce the overall shape and the main features of the experimental spectra. For graphite, the position of the peaks is accurately predicted, with a small shift ($\sim$2 eV) of the peak D to lower energies. For the peak B, the calculation predicts a double-peak structure, which is not resolved in the experimental spectrum. All the structures appearing in the calculated spectra are sharper and more pronounced. This can be attributed, at least partially, to the finite momentum-transfer resolution of ± 0.25 a.u., which is not taken into account in the calculated spectra. On the other hand, the directionally averaged simulated spectra are computed from a finite number of directional spectra. In the calculated LIG spectra, the structures above the σ^* excitation peak are predicted at slightly lower energies in comparison to the measured spectra. Regarding the structures of A, B, and C, results from present calculations are consistent with density functional theory (DFT) calculations[6] of the C $1s$ ELNES spectra for graphite and LiC_6. Within the limits of the dipole selection rule, the IXS spectra of $q||c$-axis and of $q\perp c$-axis probe unoccupied π and σ states, respectively.[29] The projections of the calculated spectra [see Fig. 1(b)] reveal that the observed features above the σ^* threshold arise mainly from transitions to unoccupied σ^* bands, with the exception of the region between about 310 and 320 eV, where σ^* and π^* contributions are comparable. While present IXS measurements, also early IXS[8,12] and EELS results,[10] show a less intense but indeed well marked π^* excitation peak in the spectrum of stage-I LIG in relation to that of graphite, DFT calculations, in both the present and in Ref. 6, predicting a strongly suppressed π^* peak. This could be attributed to a charge transfer to unoccupied π^* bands of graphite not as strong as that predicted for a fully lithiated graphite.

In Fig. 3, the difference between the energy position of the C $1s$ σ^* and π^* thresholds is displayed. The threshold separation, which is independent of the alignment methodology of the energy scale of the calculated spectra, allows a direct experiment-theory comparison. Despite small deviations (maximum discrepancy 9% for LiC_6), experimental and theoretical results show a diminishing separation between σ^* and π^* thresholds for the increasing Li content. This behavior is consistent with results from DFT calculations of ELNES spectra for the three inequivalent C sites in the LiC_{18} system,[6] which showed a decreasing shift of the σ^* threshold with increasing distance from the C sites to the intercalated Li atom.

In order to probe the empty electronic states at the Li site, Li $1s$ IXS spectra were measured in stage-II and stage-I lithiated graphite samples. The extracted Li $1s$ spectra from the whole LIG spectra (see the supplementary material for the extraction procedure) are presented in Fig. 2, along with the reference spectra from the Li metal. Relative to metallic Li, a clear shift towards higher energies of the onset of dipole-allowed transitions to empty states of high DOS can be observed for intercalated Li in both LIG systems. This chemical shift has been related to the ionic nature of the intercalated Li in stage-I LIG.[7] On the other hand, the maximum of the Li $1s$ spectra remains around the same energy region. Our results confirm these general trends of the Li core spectra in stage-I LIG, observed in previous IXS studies,[8,12] but are in disagreement with the EELS results from Hightower *et al.*,[10] which indicated a definite metallic character of Li intercalated in graphite. Results from a more recent EELS study,[7] which was carried out under optimized experimental conditions to minimize electron-beam induced damage of the samples, revealed the expected ionic nature of the intercalated Li.

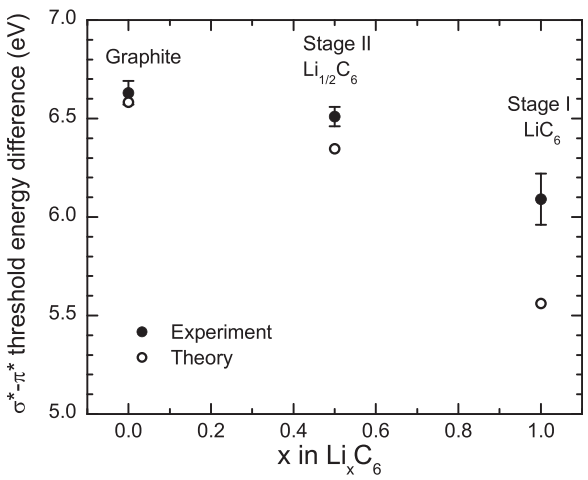

FIG. 3. C $1s$ σ^*–π^* threshold energy difference as a function of the Li content from the measured (solid circles) and simulated (open circles) IXS spectra.

Despite similarities in the shape of the Li 1*s* IXS spectra of stage-I and stage-II LIG, differences in the intensity of some spectral features can be distinguished. Above the onset of Li 1*s* excitations, a slight increment in spectral weight around 56 eV can be seen in stage-II in comparison to the stage-I spectrum. This weak spectral feature is reproduced by DFT-simulated ELNES spectra[6] of $Li_{1/2}C_6$ and LiC_6, being more prominent for the former, in consistency with the IXS measurements. A similar feature was observed in the Li 1*s* IXS spectrum of fully lithiated HOPG for $\mathbf{q}||c$-axis.[11] This structure has been attributed to transitions to bands derived from C π^* states of high DOS near the *M* point, located just above the Fermi level.[11] The larger spectral weight of this structure in the stage-II IXS spectrum could be an indication of a stronger overlap between Li core states and C-derived π^* states for $Li_{1/2}C_6$ than for LiC_6.

Concerning the fine structure in the Li 1*s* spectra, peaks, and shoulders at 61, 63, 66, and 69 eV (labeled A to D, respectively, in Fig. 2) are distinguishable in the stage-I LIG spectrum at a close inspection. These features can be well identified with those observed in a symmetry-resolved IXS spectra.[11] Spectral features at nearly the same positions were also reported from Li-core EELS spectra.[7,14] These features can be associated with structures of the projected density of unoccupied states at the Li site, according to the DOS calculations of Wang *et al.*[7] Feature B was assigned to transitions to states of high DOS of σ-type bands near the *M* point,[11] which have a large overlap with the Li core states. The depletion of spectral weight at peak B for stage-II LIG suggests that changes in the so-called interlayer states[15,30,31] of σ symmetry are occurring when going from lithiation stage I to II. Despite a small shifting of the feature positions, the experimental structures are reproduced by calculated Li 1*s* ELNES spectra of LIG systems.[6] In that theoretical work, a peak at ~69 eV was predicted for $Li_{1/2}C_6$ but not for LiC_6, while present measurements show a small peak at 69 eV in both spectra. This feature can therefore not be used to identify unambiguously the presence of the lithiation stage-II, as suggested in Ref. 6. The measured feature D in stage-I LIG might be identified with the predicted peak at ~71 eV for LiC_6, which, on the other hand, was not predicted for $Li_{1/2}C_6$. It is worth mentioning that all simulated spectra in Ref. 6 were artificially shifted by the same offset of 56 eV, thus the identification between predicted and measured structures is not conclusive.

In conclusion, our 1*s* core-excitation spectra from IXS support the invariance of the π^* excitation threshold upon Li intercalation both in stage-I and stage-II lithiated graphite. A lithiation-stage dependent shift of the σ^* threshold was observed, which appears as the clearest fingerprint for phase identification in core-electron excitation spectra. Several spectral features above the C 1*s* thresholds were observed and associated with transitions to unoccupied states of σ symmetry. The observed chemical shift of the Li *K*-edge suggests an ionic character of the intercalated Li also in stage-II LIG, which is qualitatively consistent with a predicted charge of $+0.86e$ on the Li atom in stage-II LIG.[32] Since the observed changes in the Li 1*s* near-edge structures of the two investigated LIG systems are not as pronounced and, additionally, some uncertainties originated by the extraction procedure may be expected; spectral features of the Li 1*s* spectra seem to be not a good candidate for a precise phase identification, as suggested by a theoretical study.[6] Present results provide further valuable information towards lithiation-stage studies in graphite electrodes by *in situ* experiments using inelastic scattering of hard X-rays by core-electron excitations.

See supplementary material for details about sample preparation, calculations, and data processing.

This work was supported by PIO Conicet-YPF 3855/15, PID Conicet 11220110100992 and 11220150100624, program BID-Foncyt (PICT 2012-2324 and 2015-1605), SeCyT-UNC and LNLS (Brazilian Synchrotron Light Laboratory), CNPEM/MCTI. This work used the Mendieta Cluster from CCAD-UNC, which is a part of SNCAD-MinCyT, Argentina.

[1]N. Nitta, F. Wu, J. T. Lee, and G. Yushin, Mater. Today **18**, 252 (2015).
[2]M. N. Obrovac and V. L. Chevrier, Chem. Rev. **114**, 11444 (2014).
[3]J. R. Dahn, Phys. Rev. B **44**, 9170 (1991).
[4]T. Ohzuku, Y. Iwakoshi, and K. Sawai, J. Electrochem. Soc. **140**, 2490 (1993).
[5]N. A. W. Holzwarth, S. G. Louie, and S. Rabii, Phys. Rev. B **28**, 1013 (1983).
[6]J. T. Titantah, D. Lamoen, M. Schowalter, and A. Rosenauer, Carbon **47**, 2501 (2009).
[7]F. Wang, J. Graetz, M. Sergio Moreno, C. Ma, L. Wu, V. Volkov, and Y. Zhu, ACS Nano **5**, 1190 (2011).
[8]M. Balasubramanian, C. S. Johnson, J. O. Cross, G. T. Seidler, T. T. Fister, E. A. Stern, C. Hamner, and S. O. Mariager, Appl. Phys. Lett. **91**, 031904 (2007).
[9]A. Braun, H. Wang, J. Shima, S. S. Lee, and E. J. Cairns, J. Power Sources **170**, 173 (2007).
[10]A. Hightower, C. C. Ahn, B. Fultz, and P. Rez, Appl. Phys. Lett. **77**, 238 (2000).
[11]W. Schülke, K.-J. Gabriel, A. Berthold, and H. Schulte-Schrepping, Solid State Commun. **79**, 657 (1991).
[12]W. Schülke, A. Berthold, A. Kaprolat, and H.-J. Güntherodt, Phys. Rev. Lett. **60**, 2217 (1988).
[13]A. Mansour, S. E. Schnatterly, and J. J. Ritsko, Phys. Rev. Lett. **58**, 614 (1987).
[14]L. A. Grunes, I. P. Gates, J. J. Ritsko, E. J. Mele, D. P. DiVincenzo, M. E. Preil, and J. E. Fischer, Phys. Rev. B **28**, 6681 (1983).
[15]T. Fauster, F. J. Himpsel, J. E. Fischer, and E. W. Plummer, Phys. Rev. Lett. **51**, 430 (1983).
[16]G. K. Wertheim, P. M. Th, M. Van Attekum, and S. Basu, Solid State Commun. **33**, 1127 (1980).
[17]W. Eberhardt, I. T. McQovern, E. W. Plummer, and J. E. Fisher, Phys. Rev. Lett. **44**, 200 (1980).
[18]S. B. Dicenzo, S. Basu, and G. K. Wertheim, Synth. Met. **3**, 139 (1981).
[19]V. Stancovski and S. Badilescu, J. Appl. Electrochem. **44**, 23 (2014); R. Baddour–Hadjean and J. P. Pereira–Ramos, Chem. Rev. **110**, 1278 (2010).
[20]C. Sole, N. E. Drewett, and L. J. Hardwick, Faraday Discuss. **172**, 223 (2014); J. Zou, C. Sole, N. E. Drewett, M. Velický, and L. J. Hardwick, J. Phys. Chem. Lett. **7**, 4291 (2016).
[21]W. Schülke, *Electron Dynamics by Inelastic X–Ray Scattering* (Oxford University Press, Oxford, 2007).
[22]S. Huotari, C. J. Sahle, C. Henriquet, A. Al–Zein, K. Martel, L. Simonelli, R. Verbeni, H. Gonzalez, M. C. Lagier, C. Ponchut, M. Moretti Sala, M. Krischa, and G. Monaco, J. Synchrotron Rad. **24**, 521 (2017).
[23]F. A. Lima, M. E. Saleta, R. J. S. Pagliuca, M. A. Eleotério, R. D. Reis, J. Fonseca Júnior, B. Meyer, E. M. Bittar, N. M. Souza–Neto, and E. Granado, J. Synchrotron Rad. **23**, 1538 (2016).
[24]H. Petersen, Phys. Rev. Lett. **35**, 1363 (1975).
[25]H. Nagasawa, S. Mourikis, and W. Shülke, J. Phys. Soc. Jpn. **58**, 710 (1989).

[26]J. T. Titantah and D. Lamoen, Phys. Rev. B **72**, 193104 (2005).
[27]C. Gougoussis, M. Calandra, A. Seitsonen, C. Brouder, A. Shukla, and F. Mauri, Phys. Rev. B **79**, 045118 (2009); M. Taillefumier, D. Cabaret, A. M. Flank, and F. Mauri, *ibid.* **66**, 195107 (2002).
[28]P. Giannozzi, S. Baroni, N. Bonini, M. Calandra, R. Car, C. Cavazzoni, D. Ceresoli, G. L. Chiarotti, M. Cococcioni, I. Dabo *et al.*, J. Phys.: Condens. Matter **21**, 395502 (2009).
[29]W. Schülke, U. Bonse, H. Nagasawa, A. Kaprolat, and A. Berthold, Phys. Rev. B **38**, 2112 (1988).
[30]M. Posternak, A. Baldereschi, A. J. Freeman, E. Wimmer, and M. Weinert, Phys. Rev. Lett. **50**, 761 (1983).
[31]N. A. W. Holzwarth, S. G. Louie, and S. Rabii, Phys. Rev. B **30**, 2219 (1984).
[32]S. Krishnan, G. Brenet, E. Machado–Charry, D. Caliste, L. Genovese, T. Deutsch, and P. Pochet, Appl. Phys. Lett. **103**, 251904 (2013).